Atmos. Chem. Phys. Discuss., 7, 5013–5051, 2007
www.atmos-chem-phys-discuss.net/7/5013/2007/

Atmospheric Chemistry and Physics Discussions

Vertical profiles of lightning-produced NO_2 enhancements in the upper troposphere observed by OSIRIS

C. E. Sioris[1,2,3], C. A. McLinden[1], R. V. Martin[3,4], B. Sauvage[4], C. S. Haley[5], N. D. Lloyd[2], E. J. Llewellyn[2], P. F. Bernath[6,7], C. D. Boone[6], S. Brohede[8], and C. T. McElroy[1]

[1]Experimental Studies Sect., Environment Canada, Toronto, ON, Canada
[2]Institute of Space and Atmospheric Studies, University of Saskatchewan, Saskatoon, SK, Canada
[3]Atomic and Molecular Physics Division, Harvard-Smithsonian Center for Astrophysics, Cambridge, MA, USA
[4]Department of Physics and Atmospheric Science, Dalhousie University, Halifax, NS, Canada
[5]Centre for Research in Earth and Space Science, York University, Toronto, Ontario, Canada
[6]Department of Chemistry, University of Waterloo, Waterloo, ON, Canada
[7]Department of Chemistry, University of York, Heslington, York, UK
[8]Department of Radio and Space Science, Chalmers University of Technology, Göteborg, Sweden

Received: 27 February 2007 – Accepted: 29 March 2007 – Published: 11 April 2007

Correspondence to: C. E. Sioris (christopher.sioris@ec.gc.ca)

Abstract

The purpose of this study is to perform a global search of the upper troposphere ($z \geq 10$ km) for enhancements of nitrogen dioxide and determine their sources. We have searched two years (May 2003–May 2005) of OSIRIS (Optical Spectrograph and Infrared Imager System) operational NO_2 data (version 2.3/2.4) to find large enhancements in the observations by comparing concentrations with those predicted by a photochemical model and by identifying local maxima in NO_2 volume mixing ratio. We find that lightning is the main production mechanism responsible for the large enhancements in OSIRIS NO_2 observations as expected. Similar patterns in the abundances and spatial distribution of the NO_2 enhancements are obtained by perturbing the lightning within the GEOS-Chem 3-dimensional chemical transport model. In most cases, the presence of lightning is confirmed with coincident imagery from LIS (Lightning Imaging Sensor) and the spatial extent of the NO_2 enhancement is mapped using nadir observations of tropospheric NO_2 at high spatial resolution from SCIAMACHY (Scanning Imaging Absorption Spectrometer for Atmospheric Chartography) and OMI (Ozone Monitoring Instrument). The combination of the lightning and chemical sensors allows us to investigate globally the role of lightning to the abundance of NO_2 in the upper troposphere (UT). This is the first application of satellite-based limb scattering to study upper tropospheric NO_2. The spatial and temporal distribution of NO_2 enhancements from lightning (May 2003–May 2005) is investigated. The NO_2 from lightning generally occurs at 12 to 13 km more frequently than at 10 to 11 km. This is consistent with the notion that most of the NO_2 is forming and persisting near the cloud top altitude in the tropical upper troposphere. The latitudinal distribution is mostly as expected. In general, the thunderstorms exhibiting weaker vertical development (e.g. $11 \leq z \leq 13$ km) extend latitudinally as far poleward as 45° but the thunderstorms with stronger vertical development ($z \geq 14$ km) tend to be located within 33° of the equator. There is also the expected hemispheric asymmetry in the frequency of the NO_2 enhancements, as most were observed in the Northern Hemisphere for the period analyzed.

ACPD

7, 5013–5051, 2007

1 Introduction

Lightning generates most of the NO_x (NO_2 and NO) in the low latitude upper troposphere (Lamarque et al., 1996) and has important consequences for atmospheric chemistry and climate (WMO, 1999; Intergovernmental Panel on Climate Change, 2001). However, considerable uncertainty remains in the magnitude of this natural source of NO_x (e.g. Price et al., 1997; Nesbitt et al., 2000). The vertical distribution of the lightning NO_x emissions also requires further study.

Of the available remote sensing techniques to observe lightning-generated NO_2 in the upper troposphere on a global scale, limb scattering is uniquely suited. Limb scattering has a tremendous advantage over solar occultation in terms of data volume and spatial coverage because the latter technique is limited to measuring only when the sun is on the horizon and in the field of view. Limb scattering provides the opportunity for profile information at high vertical resolution with global coverage. Infrared emission techniques also provide global coverage and can measure at night as well, however MIPAS (Michelson Interferometer for Passive Atmospheric Sounding), the only limb-viewing infrared emission instrument currently available, measures profiles of NO_2 with a vertical resolution 9–12 km below 16 km (Funke et al., 2004). The space borne limb scattering instruments currently capable of providing upper tropospheric NO_2 profile information are SCIAMACHY (Scanning Imaging Absorption Spectrometer for Atmospheric Chartography) (Bovensmann et al., 1999) and OSIRIS (Optical Spectrograph and Infrared Imager System) (Llewellyn et al., 2004). SCIAMACHY can measure NO_2 profiles down to the upper troposphere at low latitudes with an effective vertical resolution of ~3.3 km, dictated by coarse vertical sampling and large instantaneous field of view (2.6 km high by 110 km wide at the tangent point). OSIRIS yields NO_2 profiles with a typical vertical resolution of ~2 km (full width at half-maximum of the averaging kernel for the retrieval technique used below) at the median altitude of the observed NO_2 enhancements of 13 km.

The spectrograph of OSIRIS measures limb scattered radiation in the 280–810 nm

range with ∼1 nm spectral resolution. The instantaneous field of view is 1 km×30 km (vertical, horizontal) at the tangent point, allowing it to see through partly cloudy scenes more effectively and providing better vertical resolution than SCIAMACHY, and is ideal for global studies of vertically-structured phenomena such as NO_2 enhancements from lightning. Odin, the satellite bearing OSIRIS, has a polar sun-synchronous orbit with equator crossing times of 06:00 and 18:00 LT. SCIAMACHY, on the other hand, measures only at ∼10:15 LT. One of the advantages of the orbit of Odin is that OSIRIS can observe approximately the same volume of air in the summer hemisphere within 12 h. This advantage is exploited in this study. The related disadvantage is that OSIRIS gets poor coverage in the winter hemisphere. However, since most of the lightning occurs in the summer hemisphere, the orbit is well suited. Furthermore, with observational local times near twilight, NO_x partitioning is more balanced between NO_2 and NO in the tropical upper troposphere, leading to stronger NO_2 absorption signals compared to midday.

In this paper, we reveal the magnitude and spatial and temporal distribution of the observed enhancements and then highlight some interesting case studies.

2 Method

The retrieval of two years of NO_2 profiles from OSIRIS is a computationally intensive, time-consuming process. We start with version 2.4 NO_2 profiles retrieved operationally with a series of processors. The retrieval method for the operational NO_2 product is described in detail by Haley et al. (2004). The processing of the version 3.0 (v3.0) operational data product has been completed during the writing of this paper. This newest version contains a significant improvement: the retrievals will only extend down to cloud top, if present. We find however, that the operational algorithm for determining cloud tops, occasionally misidentifies the upper end of the stratospheric aerosol layer in the tropics as being a cloud top and thus a significant fraction of tropical upper tropospheric data is lost. Thus we use v2.3/2.4 data (available only to May 2005) and

an offline cloud top product described below to filter cloudy cases.

The operationally-retrieved profiles are compared with profiles generated by a stacked photochemical box model (McLinden et al., 2000) for the same local time, month, and latitude. The model extends down to ~10 km at all latitudes, and thus it covers the retrieval range of operational OSIRIS NO_2 (i.e. 10 to 46 km) with comparable vertical resolution (~2 km).

When

1. the observed profile exceeds the model profile by 1 order of magnitude at any altitude, or

2. the observed volume mixing ratio (VMR) at a given altitude minus its 1 σ uncertainty is greater than the VMR plus the 1 σ uncertainty for the immediately overlying layer,

the limb scan is selected and the data are reanalyzed as follows.

The first step is to check for the presence of clouds using the ~810 nm limb radiance profile. Five spectral pixels are co-added to reduce the impact of spikes in the data, which result mostly when the satellite is in the region of the south Atlantic anomaly (Heirtzler, 2002). This wavelength is the longest available with the optical spectrograph. For this wavelength, the atmosphere is optically thin even for upper tropospheric tangent heights and there is no limb radiance maximum at tangent heights (TH) above 10 km even for solar zenith angles approaching 90° for clear-sky conditions. Clouds (or aerosol layers with large optical depths) are identified when the limb radiance profile meets either of the following two conditions:

1) if a limb radiance maximum exists above the lowest tangent height, the corresponding tangent height is the cloud top height.

2) if the ~810 nm limb radiance scale height is <3.84. A 3.84 km scale height threshold is effective for detecting clouds since radiance scale heights of 4 to 7 km occur in the presence of background aerosols in the upper troposphere and lower stratosphere (UT/LS). The value was determined empirically after extensive examination of cloud

products generated with different threshold values. At lower threshold scale heights, the algorithm fails to detect thin clouds, whereas at higher threshold scale heights, more false positives are included, e.g. clouds are found when they are not present.

If both cloud identification conditions are met during a scan, the cloud top height is defined to be the higher of the two heights. Both of these conditions are conservative in the sense that minor aerosol layers, including the stratospheric Junge layer, are almost never mistaken for clouds. This point is demonstrated in Fig. 1, which shows the top height of clouds observed in the ~31 000 scans processed offline for this work. There are essentially no cloud detections, for example, at Northern Hemisphere mid-latitudes above 20 km, where the Junge layer would be detected if the cloud identification algorithm were sensitive to it.

Of interest, starting abruptly in mid February 2005 and continuing through April 2005, clouds were observed in the intertropical convergence zone (8° N–4° S) with top heights of >18.3 km. This corresponds to the Walker circulation regaining strength according to El Nino indicators such as the analysis by National Centers for Environmental Prediction (NCEP) of zonally averaged 500 mb temperature anomaly (http://www.cpc.ncep.noaa.gov/data/indices/z500t). The separation between these very high clouds and the usual high clouds observed between 14 and 18 km in the tropics is readily apparent in Fig. 1. Polar stratospheric clouds are also observed annually by OSIRIS in a period near the austral spring equinox (4 September–10 October).

The second step of the offline retrievals is to verify (and correct) the altitude registration. Newer (and more correct) pointing information is used in this study that was not available when v2.3/2.4 of the operational NO_2 product was generated. We use the tangent height of the ~305 nm limb radiance maximum (Sioris et al., 2003), also known as the "knee", to verify or correct the altitude registration. Often, no correction is required as Odin's attitude control system is working remarkably well (e.g. within 500 m) and better than expected (Murtagh et al., 2002; Sioris et al., 2003; Haley et al., 2004). The tangent height offset in any limb scan is corrected if the magnitude of the orbital median TH offset is greater than the standard deviation of the TH offsets during

the orbit, based on the approach developed for SCIAMACHY (Sioris et al., 2006).

The ~305 nm knee indicates an annual variation in the pointing offset, with a departure of ~500 m in June relative to the rest of the year, for which the mean offset is –297 m (Fig. 2). It is theorized that the June anomaly is caused by the Odin spacecraft twisting slightly as it cools due to the satellite being eclipsed from the sun by the Earth. Even if the apparent seasonal pointing drift were ignored, this error source translates to <15% error on the retrieved NO_2 concentration in the tropical upper troposphere (Haley et al., 2004), and thus this is a secondary source of error considering the magnitude of random errors (illustrated below). Assuming the TH offsets determined by the ~305 nm knee technique are valid, errors in the NO_2 profile will be even smaller since the TH grid is adjusted prior to the inversion and a June bias will be minimized.

After applying any necessary shift to the altitude registration and limiting the retrieval range based on the cloud top height, each scan is reprocessed using the algorithm described previously (Sioris et al., 2003, 2004), with modifications listed hereafter. The inversion scheme was changed to use Chahine's (1970) relaxation method at each iteration. This modification increases the frequency of successful retrievals but slows down the retrieval because a greater number of iterations are required. The advantage of this retrieval scheme is that the vertical resolution of the profiles is ~2 km, independent of altitude and the retrievals are almost completely independent of the first guess. These advantages are important for the current study because lightning-produced enhancements are relatively rare according to OSIRIS but consist of very large concentrations of NO_2 often confined in a narrow vertical range (e.g. 2 km), near the bottom of the retrieval range where an optimal estimation approach begins to smooth vertical profiles and rely on a priori information. However, judging from the agreement between the two retrieval schemes (not shown here; see Haley et al., 2004), the reliance on a climatological a priori NO_2 is not as significant an issue as the smoothing of the profiles, and both of these issues are minor.

We have added a surface albedo database (Koelemeijer et al., 2003) into the forward (radiative transfer) model, appropriate for clear-sky conditions. Clouds below the field

of view are still ignored, leading to small errors for large solar zenith angles (Sioris et al., 2003). The retrieval also assumes homogeneous atmospheric composition within an atmospheric layer, ignoring the diurnal gradients that exist between the near and far sides of the limb near twilight (McLinden et al., 2006). In assuming so, we speed up the forward modeling required at each iteration of the inversion at the cost of a minor retrieval error (<10%) in general (McLinden et al., 2006).

The retrieved profiles are examined for NO_2 enhancements. A profile is considered to contain an enhancement if, for the altitude at which an NO_2 enhancement of 1 order of magnitude was found in the operational data relative to the photochemical box model, there is both:

1. an increase relative to the immediately overlying retrieval layer in NO_2 volume mixing ratio (VMR), and
2. an increase in NO_2 slant column density at the closest tangent height underlying the enhanced layer, relative to the immediately overlying tangent height

Observed VMR enhancements are quantified by taking the difference in VMR as compared to the nearest overlying local minimum in the vertical profile of NO_2 VMR. Profiles are converted to VMR from NO_2 number density using air number density profiles from the atmospheric database of McLinden et al. (2002) for the appropriate latitude and month. NO_2 vertical column density (VCD) enhancements are calculated by taking the difference in retrieved NO_2 number density compared to the nearest overlying local minimum in the NO_2 number density profile. These number density enhancements are then integrated over the altitude (z) range exhibiting enhanced values. The VCD enhancements are useful for comparison with nadir viewing instruments (see below).

Some enhancements may be due to aircraft, but it is apparent that aircraft NO_x is only a minor contributor because the spatial distribution of the enhancements (Fig. 3) does not correspond to flight tracks. Another minor source of enhancements is tropopause

folds. We have filtered out many of these enhancements that occur primarily at northern mid latitudes (40–50° N in spring) by analyzing the orbital cross-sections of retrieved NO_2 (VMR as a function of latitude and altitude) to detect anomalously high NO_2 due to a strong descent of stratospheric air. The stratospheric origin of the NO_2 enhancement was confirmed by making use of NCEP 6-h tropopause data (Kalnay et al., 1996). The tropopause in each of these cases lies at a lower altitude than the climatological tropopause, indicating the intrusion of air from above (where NO_2 VMRs are significantly larger). Further analysis with a high resolution 3-D model is underway to confirm whether the enhanced NO_2 is deposited in the troposphere.

Enhancements also occur in the lower stratosphere during polar spring and are related to renoxification of the polar vortex and descent of mid-latitude air just outside the polar vortex by trapped waves (Tomikawa et al., 2003). These enhancements have been filtered out. The OSIRIS operational NO_2 data showed no large enhancements in the upper stratosphere associated with solar proton events in this time period, except on 12 April 2004 (see Randall et al., 2005).

3 Measurement biases

OSIRIS, like all limb scattering instruments, will have a clear sky sampling bias, because limb scans with towering clouds in the field-of-view are omitted from the reprocessing. However, because of the long lifetime of NO_x in the upper troposphere (~1 week, Jaegle et al., 1998), the NO_2 generated during thunderstorms can be detected after the clouds move away, tens of hours later, thus limiting the severity of this sampling bias.

There is also a spatial coverage bias as discussed in the introduction. For example, the southernmost sunlit (SZA<90°) latitude observed by OSIRIS on the descending orbital phase (morning) at the start of July, August and September 2004 is 2° S, 5° S, and 16° S, respectively. In October, both hemispheres are covered and then the coverage begins to favour the Southern Hemisphere until February, after which the Northern

Hemisphere maximal coverage returns and the annual cycle begins anew. Also, Odin is gradually precessing away from a true dawn/dusk orbit, resulting in an AM/PM bias, with more measurements in the AM, particularly in the tropics.

The month of January 2005 contains few observations as OSIRIS spent most of this month observing the mesosphere in search of polar noctilucent clouds.

4 GEOS-Chem model

We use the GEOS-Chem global 3-D chemical transport model (Bey et al., 2001) to account for the photochemical evolution and transport of NO_x. The specific simulation used here, based on GEOS-Chem version 7-02-04 (http://www-as.harvard.edu/chemistry/trop/geos), has been previously described by Sauvage et al. (2006). Briefly, the simulation is driven by assimilated meteorological data for the year 2000 from the Goddard Earth Observing System (GEOS-4) at the NASA Global Modeling and Assimilation Office (GMAO). The GEOS-Chem model includes a

detailed simulation of tropospheric ozone-NO_x-hydrocarbon chemistry as well as of aerosols and their precursors. The spatial distribution of lightning is scaled to reproduce seasonal mean lightning flash rates from the Lightning Imaging Sensor and Optical Transient Detector satellite instruments to improve the spatial distribution of lightning in the model. The timing of emissions of lightning NO_x remain linked to deep convection following the parameterization of Price and Rind (1992) with vertical profiles from Pickering et al. (1998) as implemented by Wang et al. (1998). The midlatitude and global lightning NO_x sources are 1.6 and 6 Tg N yr^{-1}, respectively, following Martin et al. (2006) and Sauvage et al. (2007).

5 Results and discussion

Figure 3 maps the enhancements in NO_2 VMR over the period 27 May 2003 to 27 May 2005 for the altitude of the maximum enhancement (i.e. typically 13 km). In all,

283 events are detected producing NO_2 VCD enhancements ranging from 3×10^{13} to 1.6×10^{15} molec/cm^2 and NO_2 VMR enhancements of 1 to 920 pmol/mol (pptv). We suggest that the lower detection limit (LDL) for NO_2 enhancements may be larger than the smallest observed enhancements, but this value depends on solar zenith angle and altitude and thus we have not omitted any of the data. Based on examination of retrieval precisions (illustrated below), the LDL appears to be on the order of 40 pptv. Nevertheless, LDLs are low considering the average observed VMR enhancement is ~125 pptv. Clearly, limb scattering, owing to its long photon paths, is very sensitive to small enhancements in NO_2 in the upper troposphere relative to nadir viewing instruments. Choi et al. (2005) observed a range of tropospheric NO_2 VCD enhancements due to lightning, all $<2.5\times10^{15}$ molec/cm^2, consistent with the upper limit of the magnitude of observed enhancements reported here.

Figures 4a–b show the NO_2 VMR at 12 km averaged over all available v2.3/2.4 and v3.0 data, respectively. The v3.0 data suffer from poor statistics in the tropics due to the filtration of "cloudy" cases, whereas v2.3/2.4 data suffer from the retrieval errors caused by the neglect of clouds. However, due to the consistency of the versions, it appears that neither problem is major. Figures 4a–b also provides a measure of the upper tropospheric background NO_2 VMR (e.g. 30 pptv over the tropical Pacific Ocean at ~06:30 LT). A similar spatial distribution of NO_2 enhancements is obtained with the GEOS-Chem 3-dimensional tropospheric chemical transport model (see Figs. 4c–d). The model simulations were sampled at 10:30 LT. This local time was chosen to clearly exclude twilight values (from the winter hemisphere) when NO_2 VMRs are much higher and changing rapidly. The OSIRIS observations are scaled to 10:30 LT using the McLinden et al. (2000) photochemical box model (see also Brohede et al., 2007). The simulated spatial pattern shown in Figs. 4d–e for z=12 km is similar at other upper tropospheric model levels but the NO_2 VMRs are smaller at higher altitudes. Figure 4e shows that at 12 km, most of the NO_2 is from lightning. Lightning NO_2 is more concentrated over Africa than over Brazil in both the OSIRIS observations and the GEOS-Chem model. Lightning flash counts from OTD (Optical Transient Detector) are

also higher over tropical Africa than South America (Christian et al., 2003). In South America, the simulated and observed UT NO_2 enhancements lie in eastern Brazil. The ten year mean flash rate over Brazil from LIS and OTD also show more lightning on the eastern half of this country (not shown). Figure 4f shows model data with GEOS-Chem sampled to match to the latitudinally and monthly dependent sampling pattern of OSIRIS. The NO_2 VMR at 12 km is weighted by the cosine of the latitude since the grid cell area decreases in the poleward direction. The weighted average is taken for the latitude region of 30° N–30° S shown in Fig. 4c for OSIRIS and Fig. 4f for GEOS_Chem in order to derive an estimate of the ratio between the observations and the simulations. The OSIRIS observations suggest, in general, larger NO_2 concentrations in the upper troposphere, but the difference between the observations and the simulations is within the uncertainty in the lightning source strength derived from other recent global analyses (e.g. Martin et al., 2007; Sauvage et al., 2007).

The NO_2 enhancements observed by OSIRIS generally occur at 12 to 13 km more frequently than at 10 to 11 km. The mean altitude of the NO_2 number density local maximum is 13.2±1.8 km (N=283). This is consistent with the notion that most of the NO_2 is forming and persisting near the cloud top altitude. Sample profiles are shown below which demonstrate this characteristic.

The latitudinal distribution is mostly as expected in the following aspect. In general, the thunderstorms exhibiting weaker vertical development (e.g. to ≤13 km) extend latitudinally as far as 45° N and ~40° S, but the thunderstorms with stronger vertical development (z≤15 km) tend to be located within 33° of the equator. There is also a hemispheric asymmetry in the frequency of the NO_2 enhancements, as most were observed in the Northern Hemisphere for the period analyzed, consistent with the GEOS-Chem simulation. The greater abundance of lightning NO_x in the Northern Hemisphere may relate to the higher fraction of land in this hemisphere as most thunderstorms occur over land.

The overall seasonality of the enhancements is shown in Fig. 5. Lightning NO_x enhancements in the North American outflow region shift from being generally south of

30° N in the boreal spring to ~40° N in midsummer. March and September correspond to the months in the Southern and Northern Hemisphere, respectively, where the sea surface temperature reaches its maximum and tropical cyclones are most intense and frequent. Hurricane Ivan appears to have been responsible for the enhancement of UT NO_2 observed on 19 September 2004 a couple of days after this hurricane had passed through the southeastern United States transitioning from a Category 1 hurricane to a tropical storm and then a tropical depression. On successive days in mid-March 2005, OSIRIS observed the 9th and 10th largest enhancements in upper tropospheric NO_2 in the 2-year period (see Table 1). These enhancements were located over the south Indian Ocean and were generated by tropical cyclone 23S (Category 2), also known as Willy. However, these were the only two tropical cyclones (see http://weather.unisys.com/hurricane/) observed by OSIRIS to generate significant lightning NO_2 in the 2-year period, indicating that hurricanes generally produce very little lightning compared to other storms, consistent with the work of Molinari et al. (1994).

As shown in Fig. 3, many upper tropospheric (UT) NO_2 enhancements lie in tropical Africa. Figure 4e shows the contribution due to lightning in the model simulations extending into Saharan Africa. NO_2 enhancements are also found in the OSIRIS observations in this desert region (Fig. 3). We hypothesize that these enhancements are from NO_2 advected from the source region of tropical western Africa since 12 of the 14 enhancements observed over Libya, Egypt and Chad are unaccompanied by coincident LIS lightning observations or any meteorological record of a thunderstorm, whereas globally, the majority of the NO_2 enhancements lie within ±4° of latitude and longitude of LIS-observed lightning occurring earlier on the same day or the previous day. Furthermore, in this region (~25° N) the circulation is dominated by the downward branch of the Hadley cell and the conditions are not favorable for cumulonimbus clouds and thunderstorms. Meteorological data (http://meteo.infospace.ru/wcarch/html/index.sht) for the given days usually show that cloud fraction is small and the air at the surface is very dry. Thus, given the similar spatial distribution to GEOS-Chem simulations of lightning-generated NO_2 (Fig. 4e), the enhancements in this region are likely a result

of advection of lightning NO_x from convective regions.

The most outstanding difference between the simulations and the observations exists in the western North Atlantic near 30° N. There is a trail of NO_2 crossing this marine region in the observations in a latitude band between 27–37° N. These observations lie at a mean altitude of 11.6±0.9 km, which corresponds very well with the altitude of 12 km chosen from the model simulations. The enhancements in the North Atlantic fall almost evenly into two narrow time periods: late summer (e.g. August) and early spring (late March to early May). Early spring enhancements in the western North Atlantic (27–37° N) of similar magnitude to those observed here were found by Choi et al. (2005). Large enhancements from lightning outflow into the western north Atlantic in early August 2004 were observed during the International Consortium for Atmospheric Research on Transport and Transformation (ICARTT) aircraft campaign (Martin et al., 2006; Hudman et al., 2007; Bertram et al., 2007). The early springtime enhancements correspond to storms with even weaker vertical development than those during late summer 2004. We are uncertain as to the reason the model is not capturing the magnitude of the lightning-produced NO_2 enhancement in the upper troposphere, but a factor of two underestimation was also observed by Martin et al. (2006) at 225 hPa ($z \cong 12$ km) in their analysis of NO_2 profiles measured by the TD-LIF instrument onboard the DC-8 during ICARTT 2004, even after increasing the northern mid-latitude lightning source to 1.6 Tg N/year (see also Hudman et al., 2007). The observed TD-LIF profiles show a greater fraction of NO_2 above 225 hPa than the model. We suspect that the low bias of the model in the North Atlantic (see Martin et al., 2006) and on a global scale (i.e. compare Fig. 4c and f) could be related to the vertical profile of lightning NO_x emissions used in the simulation.

With regard to the magnitude of the observed upper tropospheric column enhancements, they are log-normally distributed with a mode of $\sim 1.5 \times 10^{14}$ molec/cm^2 (Fig. 6). Given the single-pixel precision of SCIAMACHY tropospheric NO_2 due to spectral fitting of 8×10^{14} molec/cm^2 (Martin et al., 2006) and the OMI significance threshold of 2×10^{14} molec/cm^2 (Bucsela et al., 2006), it is apparent from Fig. 6 that a large fraction

of lightning NO_2 enhancements will be difficult to detect with the current generation of satellite nadir instruments.

6 Case studies

As stated above, 283 events, believed to be almost entirely due to lightning-generated NO_2, are found. Details for the ten largest enhancements are given in Table 1. The two largest are studied in detail, as is a third, smaller enhancement detected by four limb-viewing instruments.

6.1 Southern Indian Ocean

On the morning of 15 March 2005, the largest enhancement in the 2-year record was observed by OSIRIS over the southern Indian Ocean. LIS observed lightning on the previous afternoon (14 March 2005 at 11:21 UTC at 23.936° S, 72.074° E; see Fig. 7a). Other lightning strikes may have occurred but may not have been detected by LIS since, for example, there are gaps between swaths of successive orbits. OSIRIS detected, at 13 km, NO_2enhancements of 621±100 and 541±123 pptv in a downscan and successive upscan at (27.22° S, 76.1° E) and (27.949° S, 76.0° E), respectively. The OSIRIS spectra recorded at a tangent height of ~12 km in each scan are taken 11 s apart, translating to ~80 km in the along track direction. Using the HYSPLIT4 dispersion model (Rolph, 2003), we have determined that at 13 km, the plume of NO_x created by the aforementioned lightning flash would have traveled steadily eastward to (23° S, 75.3° E) during the 14 h separating the lightning flash and the OSIRIS observations (Fig. 7b). This trajectory puts the maximum NO_2 concentration as dispersed from the lightning flash location closer to the line of sight of OSIRIS. The upper tropospheric NO_2 column (z>11.0 km) observed by SCIAMACHY four hours later (at its local time of ~10:15) is $(1.2\pm0.3)\times10^{14}$ molec/cm^2 using the retrieval method of Sioris et al. (2004). SCIAMACHY also provides nadir imagery of tropospheric NO_2 column

abundances at high spatial resolution (e.g. 30 km×60 km). The corresponding nadir tropospheric columns (see Martin et al., 2006) for further information) are an order of magnitude larger (Fig. 7c). This suggests that most of the NO_2 enhancement lies below 11 km in this case. Possible bias in nadir tropospheric column amounts resulting from the sensitivity of the air mass factor to the assumed NO_2 profile shape can only partly explain the magnitude of the difference between the upper tropospheric NO_2 column from limb scattering and the full tropospheric column from nadir.) OSIRIS, in successive scans, observed upper tropospheric column enhancements of 1.64×10^{15} and 1.28×10^{15} molec/cm^2, an order of magnitude larger than SCIAMACHY from limb scattering but a factor of ~4 is attributable to the strong local time dependence of the NO_x partitioning near sunrise (SZA>80°) and the remaining factor of 2.5 is most likely related to the azimuthal averaging performed in the SCIAMACHY limb data analysis leading to 960 km across-track spatial resolution, judging from the large range in nadir tropospheric VCDs. This is supported by a similar factor of 2.2 which exists between the largest tropospheric VCD (1.72×10^{15} molec/cm^2) and the median tropospheric VCD (7.8×10^{14} molec/cm^2) over the SCIAMACHY nadir state (with 1σ variability of 3.3×10^{14} molec/cm^2). During the four hours between the OSIRIS and SCIAMACHY observations, the lightning NO_x plume transforms slowly into HNO_3. This chemical evolution is not taken into account and could also explain some of the differences between SCIAMACHY and OSIRIS.

This case study demonstrates two advantages of OSIRIS for remote sensing of lightning NO_2: fine across-track resolution and local times near twilight to increase NO_2 absorption signal strength, particularly from the tropopause region.

6.2 North Atlantic Ocean

The second largest VCD enhancement during the analyzed time period also occurred in March 2005. NO_2 VMR enhancements of 924±131, 502±86, and 293±95 pptv were observed in the western North Atlantic on the afternoon of 23 March 2005 and the following two mornings, respectively. LIS, with only two observing times per day, observed

peak flash rates at 05:35 UTC on 23 March 2005 off the Floridian coast as shown in Fig. 8a, but meteorological data (http://www.wunderground.com) from Titusville, FL (28.6° N, 80.8° W) indicate a thunderstorm occurred at 00:00 UTC on 23 March 2005. We calculated forward-trajectories using HYSPLIT4 (Fig. 8b) for an altitude of 12.5 km. At this altitude, the trajectory starting at 02:00 UTC on 23 March 2005 is most consistent with OSIRIS NO_2 peak heights on 23, 24 and 25 March 2005 (see below) and with the advection of the NO_2 plume visible in tropospheric column maps (Figs. 8c–d) from the Ozone Monitoring Instrument (OMI) (Levelt et al., 2006) (version 2 data, Bucsela et al., 2006). Figure 8e shows that OSIRIS captures the fact that lightning NO_x production, which appears to have originated at ∼12.5 km, descended by ∼1 km as it flowed across the North Atlantic to the observation geolocation on 24 March 2005. As well, OSIRIS observes the vertical dispersion of the NO_2 from a spike at 12 to 13 km on 23 March 2005 to a broader maximum at ∼11 km in the 24 March 2005 vertical profile. The continued descent, dispersion and evolution of the elevated-NO_x layer is apparent in the 25 March 2005 profile, which has a smaller maximum (at ≤11 km) than on the previous day and does not show any significant enhancement at 13 km.

6.3 Tropical South America

We have searched for coincidences with HALOE (Halogen Occultation Experiment), and the SCISAT instruments ACE (Atmospheric Chemistry Experiment) and MAESTRO (Measurement of Aerosol Extinction in the Stratosphere and Troposphere by Occultation) (Bernath et al., 2006). HALOE data would allow us to extend our satellite record of upper tropospheric NO_x back to 1991. Since HALOE NO_2 is only valid in the stratosphere (Gordley et al., 1996), only HALOE NO is appropriate for this. A couple of coincidences with OSIRIS NO_2 enhancements were found. One coincidence (Fig. 9) occurred on 6 August 2004 over tropical South America. The OSIRIS NO_2 enhancement at 15 km coincides with a large HALOE nitric oxide (NO) enhancement at 14.7 km. LIS had observed several lightning flashes on 5 August 2004 just north of the equator at longitudes of 71 and 62° W. The LIS flash observations were also

coincident with MAESTRO, which observed an NO_2 local maximum at 13.53 km, and ACE, which observed local maxima in NO_2 and HNO_3 volume mixing ratio at 13.8 km, and a local maximum in NO at the lowest point in that profile at 15.2 km. There are a few other cases of coincident enhancements in NO, NO_2 and/or HNO_3 between ACE, MAESTRO and OSIRIS. Thus, it appears that the SCISAT instruments can also assist in the global measurement of lightning NO_x and NO_y from space, but further investigation is required to determine whether the HALOE NO dataset can be useful for studying lightning NO_x over the past fifteen years.

7 Summary, conclusions and future work

Enhancements in upper tropospheric nitrogen dioxide are observed by OSIRIS. Most of these enhancements are found in locations near where lightning has occurred on the previous day or earlier on the same day. LIS and hourly meteorological reports from surface sites were used to locate the lightning in space and time. Many enhancements are seen by OSIRIS in consecutive limb scans or after 12 h in the downwind direction, demonstrating both the self-consistency and valuable spatio-temporal coverage of the OSIRIS observations. The SCIAMACHY and OMI tropospheric NO_2 column maps reveal the large spatial extent of enhanced NO_x generated from isolated thunderstorms, such as in the case presented above over the southern Indian Ocean.

The simulation of lightning NO_x in the upper troposphere with the GEOS-Chem chemical transport model is consistent with the enhancements observed by OSIRIS in terms of the overall spatial pattern of lightning-induced hotspots, and in the advection of lightning NO_x (e.g. across northeastern Africa from source regions such as tropical western and central Africa). As discussed above, several possible sources of high bias in the OSIRIS NO_2 observations at 12 km were removed for the purpose of comparing with the GEOS-Chem simulations. We accounted for the strong diurnal variation in the NO_2 data set of OSIRIS (which often measures near twilight) by converting all profiles to mid-morning. The sampling bias toward summer hemisphere

data was taken into account as well. Finally, stratospheric NO_2 was filtered from the observations. Nevertheless, the OSIRIS background NO_2 VMR at 12 km remains, on average, 6 to 7 ppt higher than the simulations. Thus, OSIRIS observations at 12 km could imply a 40% increase in the global lightning source strength of 6 Tg N/yr used in the GEOS-Chem simulations, at the upper limit of the uncertainty inferred from recent studies (Martin et al., 2007; Sauvage et al., 2007). It is likely that the bias relates to the assumed vertical distribution of lightning NO_x in the model. MAESTRO observations of lightning-generated NO_2 may assist in characterizing the assumed profile shape, given the ~1 km vertical resolution of this instrument.

Even though, most lightning occurs over land (Christian et al., 2003), NO_2 enhancements frequently occur over the ocean due to transport and the long lifetime of NO_x in the upper troposphere. In the Atlantic Ocean, three bands of enhanced NO_2 are observed. The first lies within a few degrees of the equator. The second appears to be a result of outflow from the southeast U.S., which starts in spring at ~25° N and moves to higher latitudes in boreal summer. Thirdly, a weaker band appears at ~20° S in austral summer following the movement of the intertropical convergence zone. In contrast, fewer upper tropospheric NO_2 enhancements are found in the Pacific and Indian Oceans and lower baseline concentrations of NO_2 are observed there, consistent with the simulations.

We will extend our case-by-case investigation of NO_2 enhancements over the full, six year data record with the next version of the operational OSIRIS NO_2 product.

Acknowledgements. The authors gratefully acknowledge the NOAA Air Resources Laboratory (ARL) for the provision of the HYSPLIT transport and dispersion model and the READY website (http://www.arl.noaa.gov/ready.html) used in this publication. NCEP reanalysis data are provided by the NOAA/OAR/ESRL PSD, Boulder, Colorado, USA, from their website at (http://www.cdc.noaa.gov/). We also thank the LIS, HALOE and OMI teams for their publicly available data. This work and the ACE mission are supported by the Canadian Space Agency and Natural Science and Engineering Research Council of Canada.

References

Bernath, P. F, McElroy, C. T., Abrams, M. C., et al.: Atmospheric Chemistry Experiment (ACE): Mission overview, Geophys. Res. Lett., 32, L15S01, doi:10.1029/2005GL022386, 2005.

Bertram, T. H., Perring, A. E., Wooldridge, P. J., et al.: Direct measurements of the convective recycling of the upper troposphere, Science, 315, 816–820, 2007.

Bey, I., Jacob, D. J., Yantosca, R. M., Logan, J. A., Field, B., Fiore, A. M., Li, Q., Liu, H., Mickley, L. J., and Schultz, M.: Global modeling of tropospheric chemistry with assimilated meteorology: Model description and evaluation, J. Geophys. Res., 106, 23 073–23 096, 2001.

Bovensmann, H., Burrows, J. P., Buchwitz, M., Frerick, J., Rozanov, S., Noël, V. V., Chance, K. V., and Goede, A. P. H.: SCIAMACHY: Mission objectives and measurement modes, J. Atmos. Sci., 56, 127–150, 1999.

Brohede, S. M., Haley, C. S., McLinden, C. A., et al.: Validation of Odin/OSIRIS stratospheric NO_2 profiles, J. Geophys. Res., in press, 2007.

Bucsela, E. J., Celarier, E. A., Wenig, M. O., Gleason, J. F., Veefkind, J. P., Boersma, K. F., and Brinksma, E. J.: Algorithm for NO_2 vertical column retrieval from the Ozone Monitoring Instrument, IEEE Trans. Geosci. Remote Sens., 44, 1245–1258, 2006.

Chahine, M. T.: Inverse problems in radiative transfer: Determination of atmospheric parameters, J. Atmos. Sci., 27, 960–967, 1970.

Choi, Y., Wang, Y., Zeng, T., Martin, R. V., Kurosu, T. P., and Chance, K.: Evidence of lightning NO_x and convective transport of pollutants in satellite observations over North America, Geophys. Res. Lett., 32, L02805, doi:10.1029/2004GL021436, 2005.

Christian, H. J., Blakeslee, R. J., Boccippio, D. J., et al.: Global frequency and distribution of lightning as observed from space by the Optical Transient Detector, J. Geophys. Res., 108(D1), 4005, doi:10.1029/2002JD002347, 2003.

Funke, B., López-Puertas, M., von Clarmann, T., et al.: Retrieval of stratospheric NO_x from 5.3 and 6.2 mm nonlocal thermodynamic equilibrium emissions measured by Michelson Interferometer for Passive Atmospheric Sounding (MIPAS) on Envisat, J. Geophys. Res., 110, D09302, doi:10.1029/2004JD005225, 2005.

Gordley, L. L., Russell III, J. M., Mickley, L. J., et al.: Validation of nitric oxide and nitrogen dioxide measurements made by the Halogen Occultation Experiment for UARS platform, J. Geophys. Res., 101, 10 241–10 266, 1996.

Haley, C. S., Brohede, S. M., Sioris, C. E., Griffioen, E., Murtagh, D. P., McDade, I. C., Eriksson,

P., Llewellyn, E. J., Bazureau, A., and Goutail, F.: Retrieval of stratospheric O_3 and NO_2 profiles from Odin Optical Spectrograph and Infrared Imager System (OSIRIS) limb-scattered sunlight measurements, J. Geophys. Res., 109, D16303, doi:10.1029/2004JD004588, 2004.
Heirtzler, J. R.: The future of the South Atlantic anomaly and implications for radiation damage in space, J. Atmos. Solar-Terr. Phys., 64, 1701–1708, 2002.
Hudman, R. C., Jacob, D. J., Turquety, S., et al.: Surface and lightning sources of nitrogen oxides over the United States: magnitudes, chemical evolution, and outflow, J. Geophys. Res., in press, 2007.
Intergovernmental Panel on Climate Change, Climate change 2001: The scientific basis, 881 pp., Cambridge University Press, Cambridge, UK, 2001.
Jaeglé, L., Jacob, D. J., Wang, Y., Weinheimer, A. J., Ridley, B. A., Campos, T. L., Sachse, G. W., and Hagen, D. E.: Sources and chemistry of NO_x in the upper troposphere over the United States, Geophys. Res. Lett., 25, 1705–1708, 1998.
Kalnay, E., Kanamitsu, M., Kistler, R., et al.: The NCEP/NCAR 40-year reanalysis project, Bull. Amer. Meteorol. Soc., 77, 437–470, 1996.
Koelemeijer, R. B. A., de Haan, J. F., and Stammes, P.: A database of spectral surface reflectivity in the range 335–772 nm derived from 5.5 years of GOME observations, J. Geophys. Res., 108(D2), 4070, doi:10.1029/2002JD002429, 2003.
Lamarque, J. F., Brasseur, G. P., Hess, P. G., and Mueller, J. F.: Three-dimensional study of the relative contributions of the different nitrogen sources in the troposphere, J. Geophys. Res., 101, 22 955–22 968, 2006.
Levelt, P. F., van den Oord, G. H. J., Dobber, M. R., Mälkki, A., Visser, H., de Vries, J., Stammes, P., Lundell, J., and Saari, H.: The Ozone Monitoring Instrument, IEEE Trans. Geosci. Remote Sens., 44, 1093–1101, 2006.
Llewellyn, E. J., Lloyd, N. D., Degenstein, D. A., et al.: The OSIRIS instrument on the Odin satellite, Can. J. Phys., 82, 411–422, 2004.
Martin, R. V., Sauvage, B., Folkins, I., Sioris, C. E., Boone, C., Bernath, P., Ziemke, J.: Space-based constraints on the production of nitric oxide by lightning, J. Geophys. Res., in press, 2007.
Martin, R. V., Sioris, C. E., Chance, K., Ryerson, T. B., Bertram, T. H., Wooldridge, P. J., Cohen, R. C., Neuman, J. A., Swanson, A. L., and Flocke, F. M.: Evaluation of space-based constraints on global nitrogen oxide emissions with regional aircraft measurements over and downwind of eastern North America, J. Geophys. Res., 111, D15308,

doi:10.1029/2005JD006680, 2006.
McLinden, C. A., McConnell, J. C., Griffioen, E., and McElroy, C. T.: A vector radiative-transfer model for the Odin/OSIRIS project, Can. J. Phys. 80, 375–393, 2002.
McLinden, C. A., Olsen, S. C., Hannegan, B. J., Wild, O., Prather, M. J., and Sundet, J.: Stratospheric Ozone in 3-D Models: A simple chemistry and the cross-tropopause flux, J. Geophys. Res., 105, 14 653–14 665, 2000.
McLinden, C. A., Haley, C. S., and Sioris, C. E.: Diurnal effects in limb scatter observations, J. Geophys. Res., 111, D14302, doi:10.1029/2005JD006628, 2006.
Molinari, J., Moore, P. K., Idone, V. P., Henderson, R. W., and Saljoughy, A. B.: Cloud-to-ground lightning in Hurricane Andrew, J. Geophys. Res., 99(D8), 16 665–16 676, 1994.
Murtagh, D., Frsik, U. , Merino, F., et al.: An overview of the Odin atmospheric mission, Can. J. Phys. 80, 309–319, 2002.
Nesbitt, S. W., Zhang, R., and Orville, R. E.: Seasonal and global NO_x production by lightning estimated from the Optical Transient Detector (OTD), Tellus, 52B, 1206–1215, 2000.
Pickering, K. E., Wang, Y. S., Tao, W. K., Price, C., and Mueller, J. F.: Vertical distributions of lightning NO_x for use in regional and global chemical transport models, J. Geophys. Res., 103(D23), 31 203–31 216, 1998.
Price, C. and Rind, D.: A simple lightning parameterization for calculating global lightning distributions, J. Geophys. Res., 97, 9919–9933, 1992.
Price, C., Penner, J., and Prather, M.: $NO_x$from lightning 1. Global distribution based on lightning physics, J. Geophys. Res., 102, 5929–5941, 1997.
Randall, C. E., Harvey, V. L., Manney, G. L., et al.: Stratospheric effects of energetic particle precipitation in 2003–2004, Geophys. Res. Lett., 32, L05802, doi:10.1029/2004GL022003, 2005.
Rolph, G. D.: Real-time Environmental Applications and Display sYstem (READY) Website (http://www.arl.noaa.gov/ready/hysplit4.html), NOAA Air Resources Laboratory, Silver Spring, MD, 2003.
Sauvage, B., Martin, R. V., van Donkelaar, A., Liu, X., Chance, K., Jaeglé, L., Palmer, P. I., Wu, S., and Fu, T. M.: Remote sensed and in situ constraints on processes affecting tropical tropospheric ozone, Atmos. Chem. Phys., 7, 815–838, 2007, http://www.atmos-chem-phys.net/7/815/2007/.
Sioris, C. E., Haley, C. S., McLinden, C. A., et al.: Stratospheric profiles of nitrogen dioxide observed by Optical Spectrograph and Infrared Imager System on the Odin satellite, J. Geo-

phys. Res., 108(D7), 4215, doi:10.1029/2002JD002672, 2003.
Sioris, C. E., Kurosu, T. P., Martin, R. V., and Chance, K.: Stratospheric and tropospheric NO2 observed by SCIAMACHY: First results, Adv. Space Res., 34(4), 780–785, 2004.
Sioris, C. E., Kovalenko, L. J., McLinden, C. A., et al.: Latitudinal and vertical distribution of bromine monoxide in the lower stratosphere from SCIAMACHY limb scattering measurements, J. Geophys. Res., 111, D14301, doi:10.1029/2005JD006479, 2006.
Tomikawa, Y. and Sato, K.,: Trapped waves in the edge region of stratospheric polar vortices, J. Geophys. Res., 108(D2), 4047, doi:10.1029/2002JD002579, 2003.
Wang, Y., Jacob, D. J., and Logan, J. A.: Global simulation of tropospheric O3-NO_x-hydrocarbon chemistry, 1. Model formulation, J. Geophys. Res., 103, 10 713–10 726, 1998.
World Meteorological Organization: Scientific Assessment of Ozone Depletion: 1998, Geneva, Switzerland, 1999.

Table 1. Top ten enhancements in upper tropospheric column NO2 (in molec/cm^2), listed in descending order of column enhancement (see method for details). The difference in NO2 VMR between the local maximum and the nearest overlying local minimum is "dVMR".

dd	mm	yyyy	z (km)	lat (°)	lon (°)	AM/ PM	VCD ($\times 10^{14}$ molec cm^2)	VMR (pptv)	dVMR (pptv)	Remark, LIS info
15	03	2005	13	–26	76	AM	16.4	710	621	S. Indian Ocean; LIS: 11:21 UTC [14/03/2005] (–23.936, 72.074) (see Sect. 6.1)
24	03	2005	11	27	–46	AM	15.1	590	502	Atlantic; (see Sect. 6.2)
15	03	2005	13	–29	76	AM	12.8	633	541	S. Indian Ocean; LIS: 11:21 UTC [14 March 2005] (–23.936, 72.074)
23	03	2005	13	32	–59	PM	10.5	1015	924	Atlantic; (see Sect. 6.2)
12	03	2005	15	–29	56	AM	10.2	901	851	S. Indian Ocean; LIS: 14:03 UTC [11 March 2005] (–24.631, 47.222)
04	06	2004	11	–7	9	AM	10.0	314	231	Atlantic; LIS: 12:17 UTC [3 June 2004] (–1.451, 7.329)
01	04	2005	11	30	–72	PM	8.31	349	259	Atlantic; LIS: 02:09 UTC [1 April 2005] (31.389, –79.425)
04	05	2004	11	–7	13	AM	8.27	312	222	Angola; no coinc. LIS obs.; no lightning or thunder at ground
16	03	2005	13	–17	101	AM	8.19	301	275	S. Indian Ocean; no LIS lightning, tropical cyclone Willy (see Sect. 5)
15	03	2005	13	–16	103	AM	8.15	286	232	S. Indian Ocean; no LIS lightning, tropical cyclone Willy

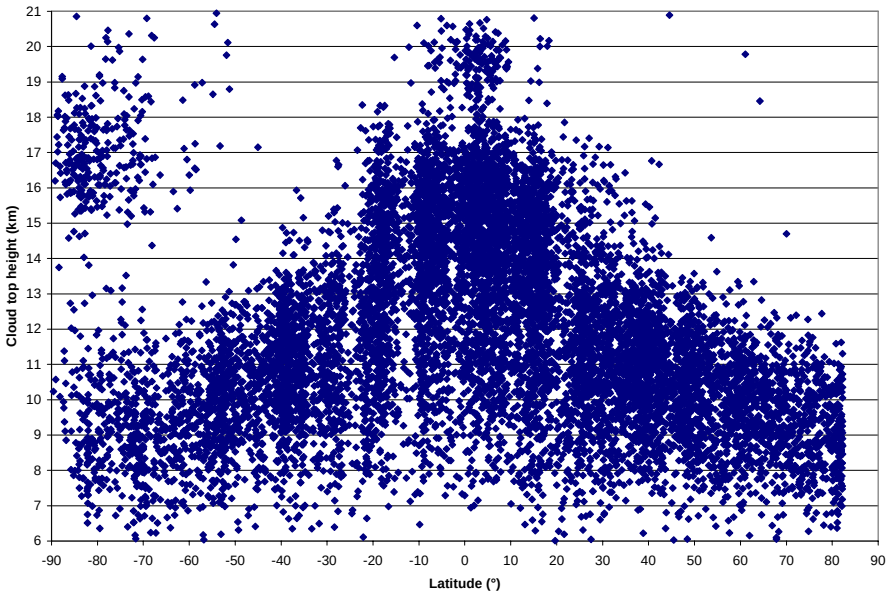

Fig. 1. Cloud top heights observed by OSIRIS from ~1100 selected orbits during the period of investigation (27 May 2003–27 May 2005). Orbits are included from each month. Polar stratospheric clouds are observed in austral spring at high latitudes at ~17 km.

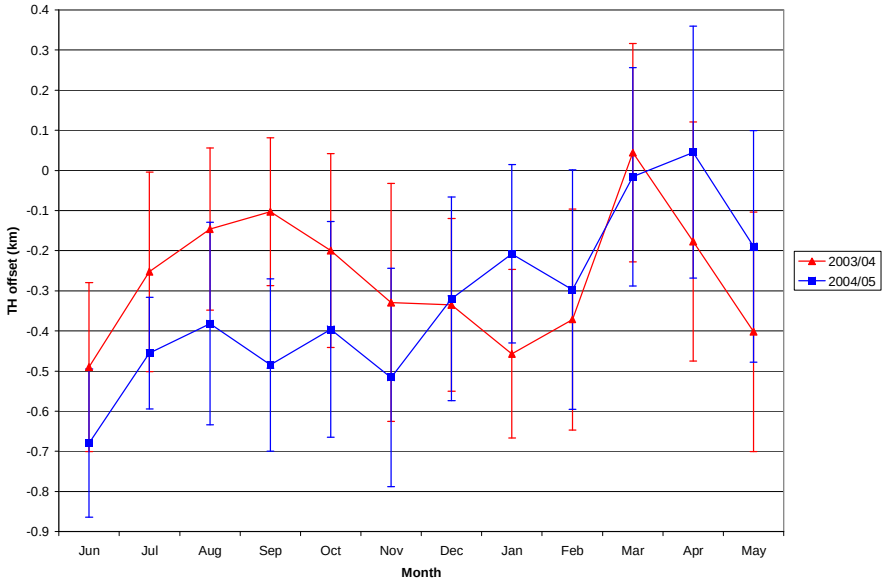

Fig. 2. Monthly mean tangent height offset for OSIRIS as inferred from the ~305 nm knee (Sioris et al., 2003). An annual pattern is detected in the two year period of investigation. The error bars show 1 standard deviation about the monthly mean.

ACPD
7, 5013–5051, 2007

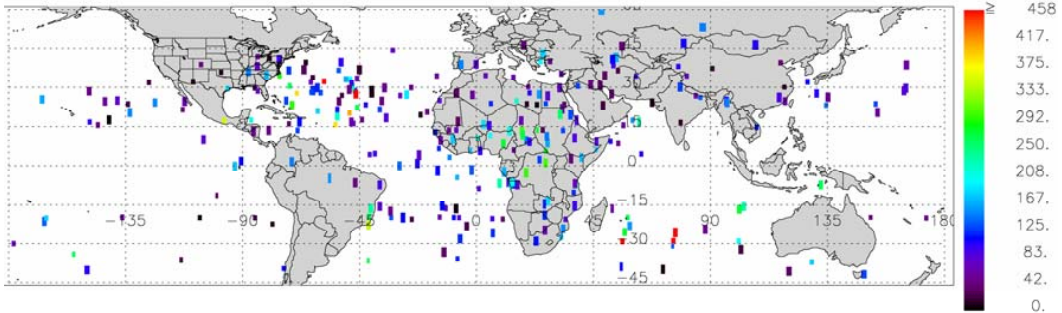

Fig. 3. Map of upper tropospheric NO_2 volume mixing ratio enhancements detected by OSIRIS during the period 27 May 2003 to 27 May 2005. Colour is used to indicate the magnitude of the enhancements in pptv. The longitudinal extent of each OSIRIS spatial pixel has been extended by 0.5° to the east and west of the pixel center for illustrative purposes.

ACPD
7, 5013–5051, 2007

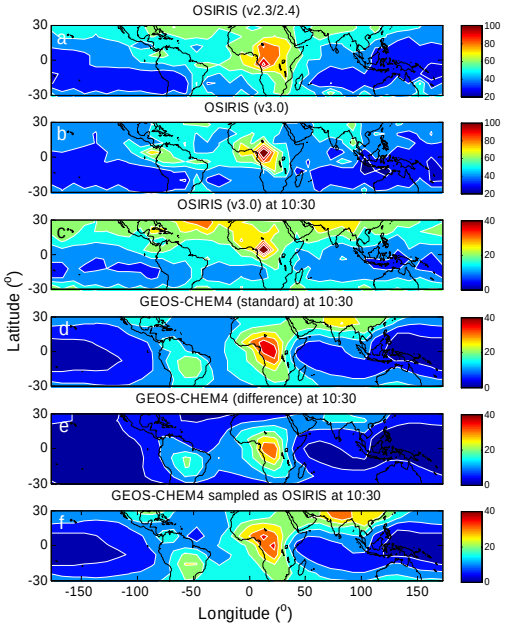

Fig. 4. OSIRIS operational NO_2 VMR (v2.3/2.4) at 12 km, in pptv; AM data only, averaged over all available data (2001 to 2007) and gridded on 8°×10° (latitude, longitude), **(b)** same as **(a)** but for v3.0, **(c)** same as (b), but with different colour scale and with diurnal scaling to 10:30 LT and with stratospheric points removed by defining the tropopause (see McLinden et al., 2000) as the lowest altitude with 150 ppbv of OSIRIS O3 (v3.0), **(d)** map of annual mean NO_2 VMR including lightning at z=12 km for the year 2000, calculated for 10:30 LT with the GEOS-Chem model. **(e)** same as d) except the difference is taken from a model run without lightning to isolate the contribution from lightning, **(f)** same as (e), except that, an attempt was made to order to make the temporal sampling of GEOS-Chem consistent with that of OSIRIS. The monthly mean model data was weighted as a function of latitude by the fraction of all OSIRIS data points (at the same latitude) that occurred in that month in order to make the temporal sampling of GEOS-Chem consistent with that of OSIRIS.

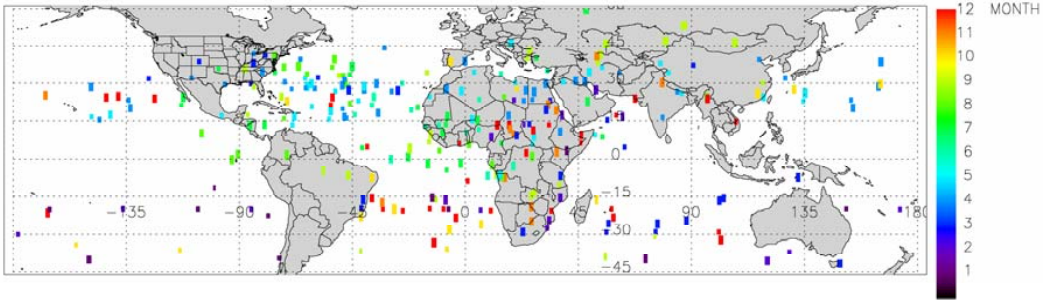

Fig. 5. Location of OSIRIS UT NO_2 enhancements as a function of month over the 2 year period (May 2003–May 2005). December, for example, is the 12th month and thus, observation locations are in red. The longitudinal extent of each OSIRIS spatial pixel has been extended by 0.5° to the east and west of the pixel center for illustrative purposes.

ACPD
7, 5013–5051, 2007

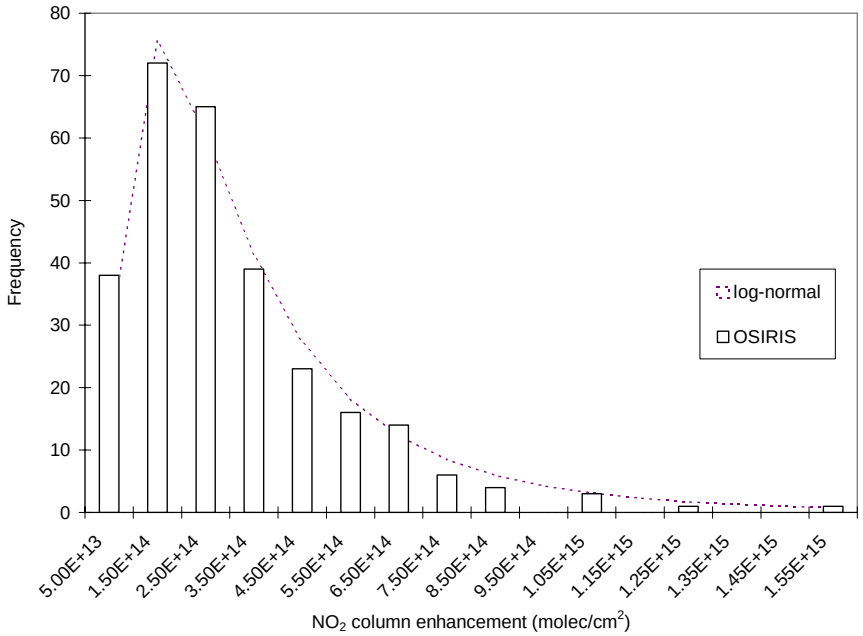

Fig. 6. Distribution of OSIRIS UT NO_2 column enhancements due to lightning is well described (r^2=0.9754) by a 3-parameter log-normal distribution. Bin midpoint values are plotted along the x-axis.

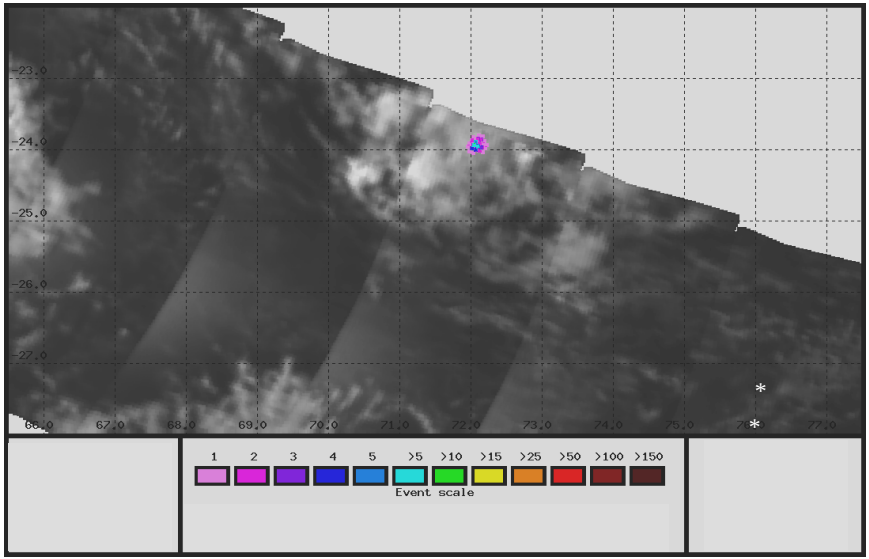

Fig. 7a. Lightning imagery from LIS (http://thunder.msfc.nasa.gov) showing an isolated storm cell at ~11:20 UTC on 14 March 2005, one day before OSIRIS observed enhancements in NO_2 of 620 and 540 pptv in successive limb scans at 27.22° S, 76.1° E, and 27.95° S, 76.0° E (indicated by white asterisks).

ACPD
7, 5013–5051, 2007

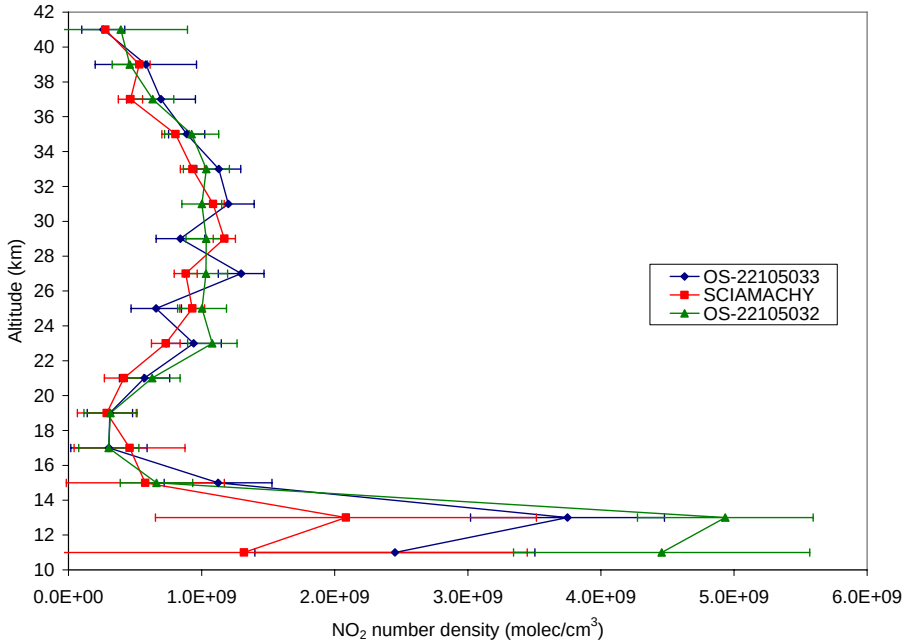

Fig. 7b. Comparison of NO_2 profiles from SCIAMACHY (25.923° S, 76.002° E, SZA=44° AM) and OSIRIS on 15 March 2005 after nearby lightning flashes hours earlier led to large enhancements in NO_2. OSIRIS scans 32 and 33 are at (27.22° S, 76.1° E, SZA=88.09° AM) and (27.949° S, 76.0° E, SZA=88.59° AM), respectively, for TH≅13 km. All three profiles have been converted to SZA=88.59° AM to account for diurnal variation using a photochemical model (McLinden et al., 2000; see also Brohede et al., 2007).

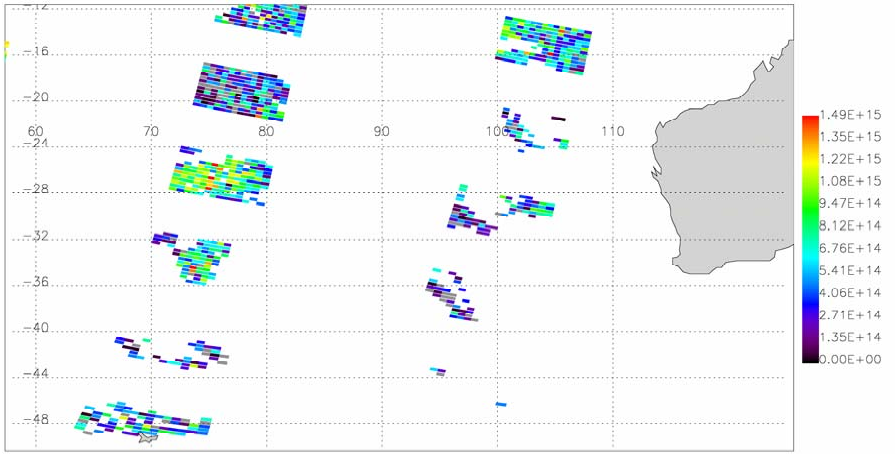

Fig. 7c. SCIAMACHY tropospheric NO_2 column (molec/cm^2) map on 15 March 2005, after filtering ground pixels with cloud radiance fraction of >0.5. The NO_2 enhancement stretches over several degrees of longitude (72–79° E) and latitude (25–28° S). Background tropospheric NO_2 column abundances (<10^{15} molec/ cm^2) surround the enhancement to the east, north and south and are also observed in the surrounding nadir states. From coincident SCIAMACHY limb scattering observations, the highest clouds in this region had tops at ~5 km.

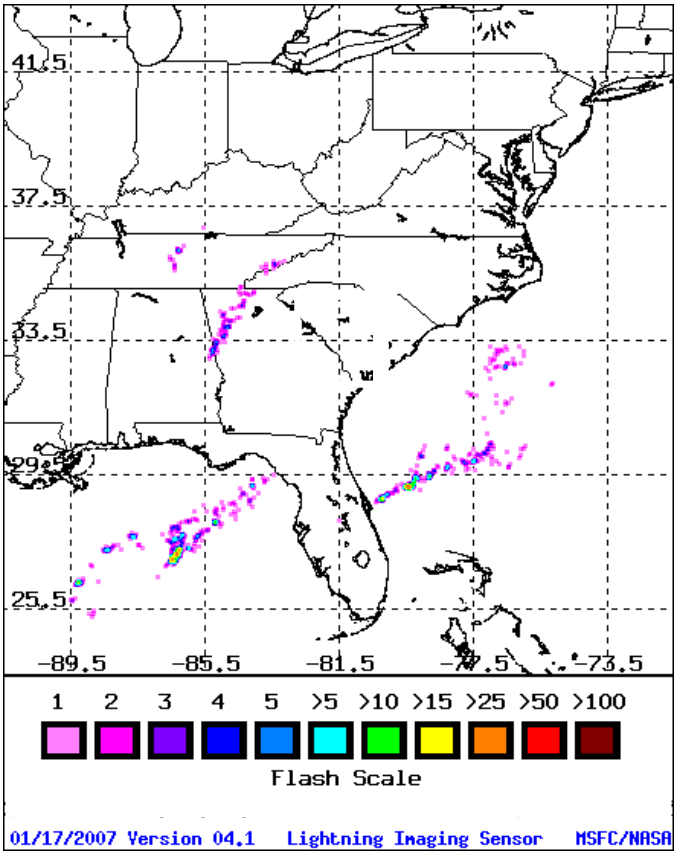

Fig. 8a. Lightning imagery from LIS showing lightning extending out over the Atlantic northeast of Florida at 05:35 UTC on 23 March 2005.

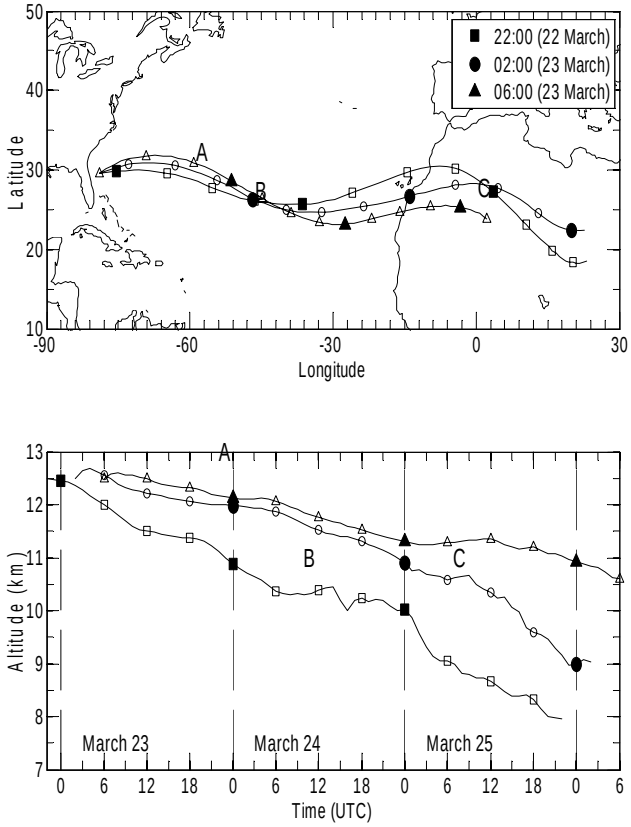

Fig. 8b. 72 h forward trajectories for start geolocation of z=12.5 km, 29.5° N, 79° W. Start times of the trajectories are shown in the legend. The bottom panel shows the descent in altitude as the air parcel moves forward in time from off the coast of northern Florida, coincident with the observed thunderstorm. A, B, C indicate the position in time and space of the series of enhancements observed by OSIRIS.

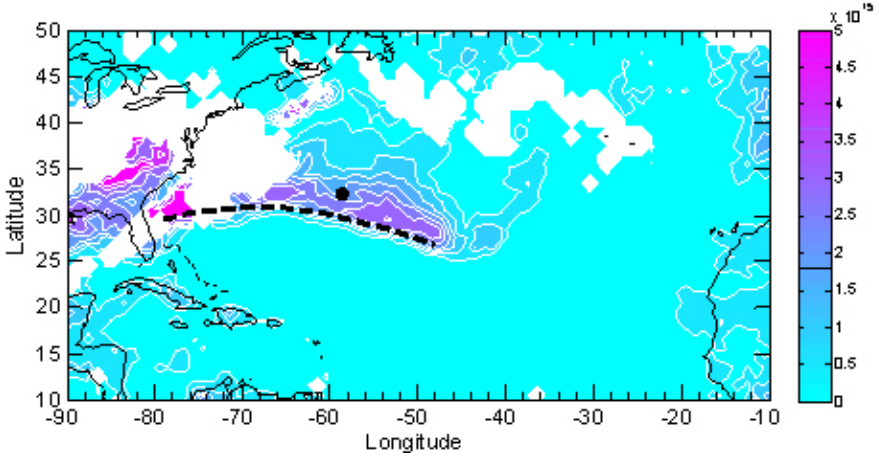

Fig. 8c. Tropospheric column NO_2 (molec/cm^2) from OMI on 23 March 2005 showing a plume of NO_2 transported along the trajectory starting at 02:00 UTC on 23 March 2005, also shown in Fig. 8b. The trajectory during the same calendar day (UTC) is shown. The filled black circle represents the location of the OSIRIS profile from the same calendar day (shown below). Cloudy OMI data have been filtered using a cloud fraction threshold of 0.5. The local time of the OMI measurements is approximately 13:30.

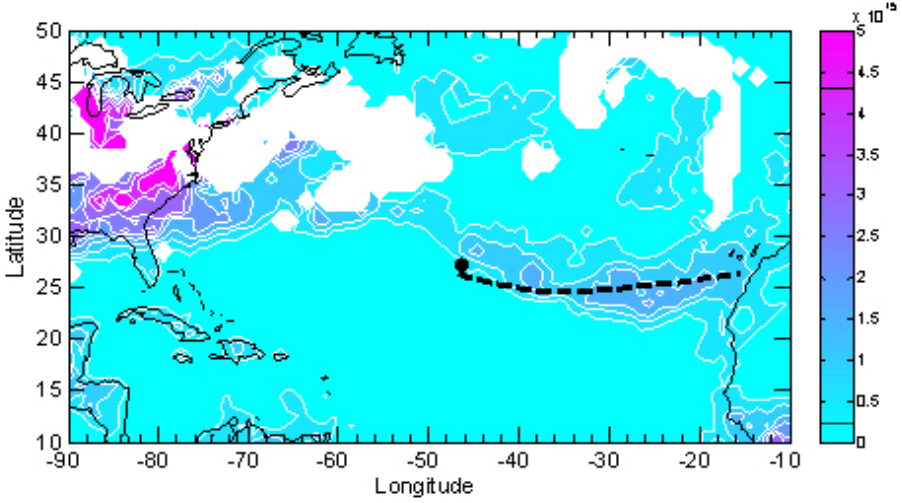

Fig. 8d. Same as (c), except for 24 March 2005. OMI data was not available on 25 March 2005 for the Atlantic region.

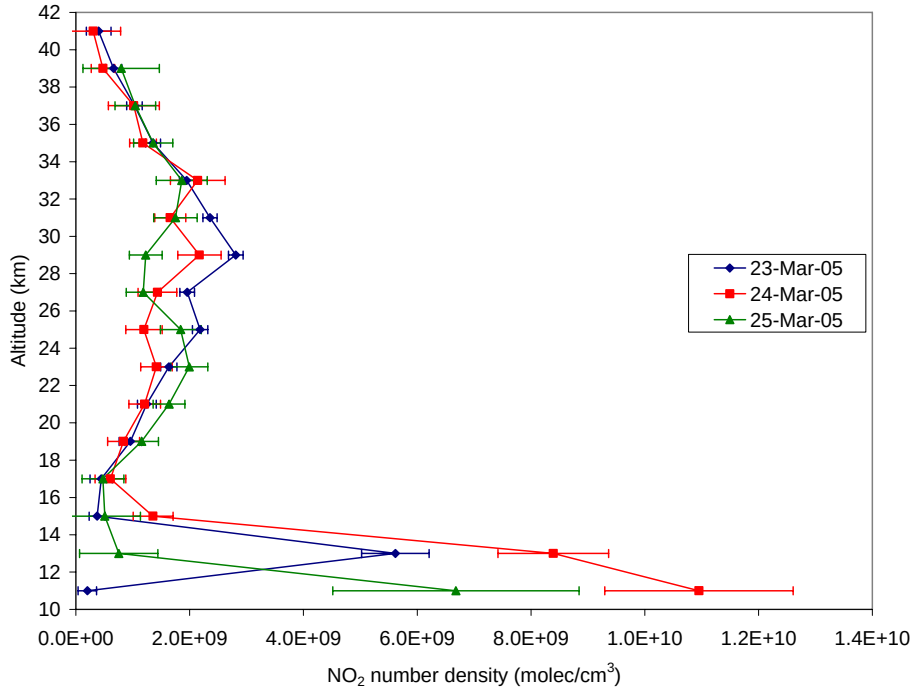

Fig. 8e. NO_2 number density profiles observed by OSIRIS at 32.3° N, 58.7° W on 23/03/2005 (SZA=89.643° PM), at 27.3° N, 46.4° W on 24 March 2005 (SZA=80.746° AM), and at 27.7° N, 0.3° E on 25 March 2005 (SZA=80.563° AM). The profiles on 24–25 March 2005 have been scaled to SZA=89.643° PM to allow for comparison of the profiles without diurnal differences in NO_x partitioning.

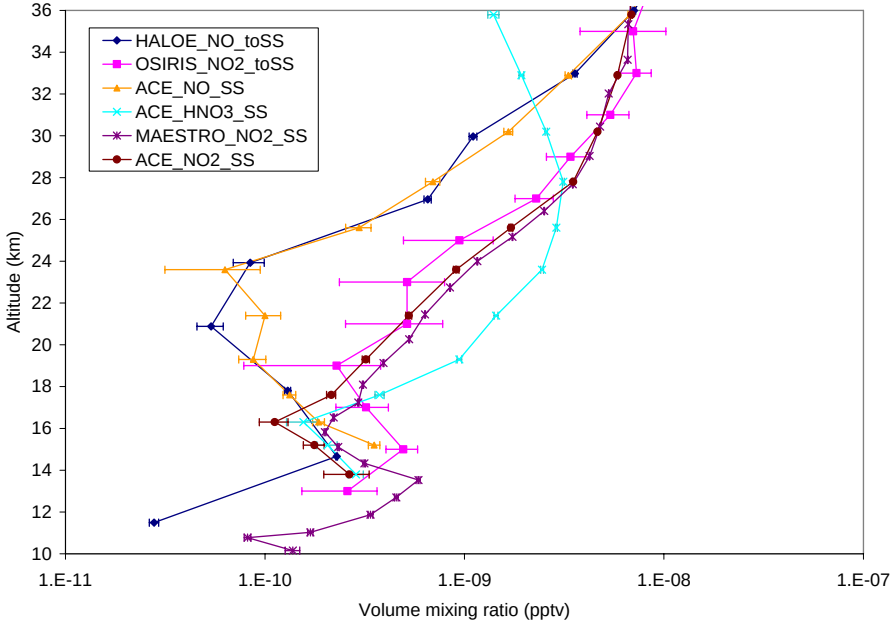

Fig. 9. Coincident profiles of odd nitrogen species observed by four satellite instruments on 6 August 2004 showing enhanced mixing ratios in the upper troposphere shortly after several nearby lightning strikes in tropical South America. MAESTRO and ACE observed NO_2 while the latter also observed HNO_3 and NO at local sunset (3.3° N, 71.7° W). HALOE NO (3.7° N, 58.8° W) was measured at local sunrise but has been converted to sunset as has OSIRIS NO_2 (2° N, 71° N) through the use of a photochemical model (McLinden et al., 2000).